

POWER LOSS CALCULATION IN SEPARATED AND COMMON BEAM CHAMBERS OF THE LHC

C. Zannini and G. Rumolo, CERN, Geneva
 G. Iadarola, Università di Napoli Federico II, Napoli; CERN, Geneva

Abstract

The performance of 25 ns beams in the LHC is strongly limited by the electron cloud. To determine the amount of electron cloud in the cold sections of the machine, it is very important to be able to disentangle the beam induced heating due to the beam coupling impedance from that attributable to electron cloud. This paper will focus on the calculation of the first contribution. First, the impedance model used for the calculation of the beam induced power loss is briefly discussed. Then, the methods for the calculation of the beam induced power loss in regions with one or two beams are also described. Finally, the calculated power loss is compared with the measured heat loads for both 25 and 50 ns beams in both the LHC arcs and in the inner triplets (ITs).

INTRODUCTION

The beam induced heating of the LHC beam screens (see Fig. 1) is of special concern in cold magnets, where it could exceed the cooling capacity of the cryogenic system and lead to a quench. This paper aims to disentangle the beam induced heating due to the beam coupling impedance from that attributable to electron cloud and will focus on the calculation of the first contribution.

BEAM COUPLING IMPEDANCE MODEL OF THE LHC BEAM SCREEN

The beam screen used in the LHC main dipoles (see Fig. 1) is a pipe made of 1 mm thick ultra-low magnetic permeability stainless steel (SS) coated on its inner surface with a 50 μm layer of high electrical conductivity Copper (Cu) to minimize resistive wall losses. First studies on the beam screen impedance model can be found in [1]. More detailed studies were later conducted and summarized in [2]. Recently a more realistic impedance model based on CST 3D Wakefield simulations [3] has been developed [4]. Resorting to the simulation scaling technique [4] the longitudinal and transverse beam coupling impedance of the LHC beam screen including the effect of the weld have been simulated from 1 kHz up to several GHz.

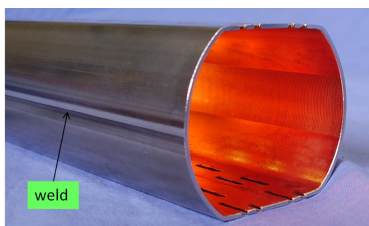


Figure 1: The LHC beam screen as it is built and installed. Courtesy of N. Kos

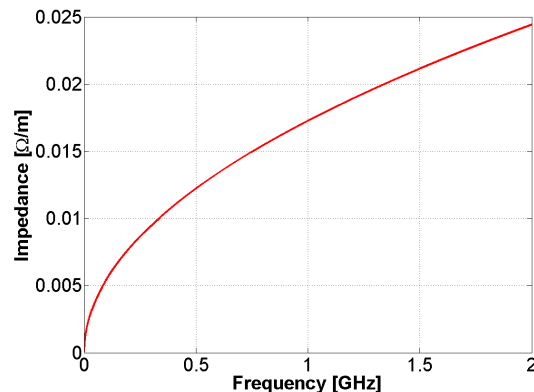


Figure 2: Real part of the longitudinal impedance of the arc beam screen per meter length

BEAM INDUCED POWER LOSS

The power lost by a beam passing with revolution frequency $f_0 = \frac{\omega_0}{2\pi}$ through a device having longitudinal impedance $Z_{||}(\omega)$ can be expressed as [4]:

$$\Delta W = (f_0 e N_{\text{beam}})^2 \sum_{p=-\infty}^{p=\infty} \left(\left| \bar{\Lambda}(p\omega_0) \right|^2 \text{Re} [Z_{||}(p\omega_0)] \right) \quad (1)$$

where e is the charge of the particle, N_{beam} is the beam intensity (total number of particles in the beam) and $\bar{\Lambda}(p\omega_0)$ is the normalized beam spectrum.

Power Loss in the Arc Beam Screen

The beam induced power loss in the arc beam screen can be analytically calculated by using Eq. (1). The real part of the longitudinal impedance of the arc beam screen including also the effect of the weld is shown in Fig. 2.

The beam spectrum is analytically calculated by using beam measurements information (bunch pattern, bunch intensities and bunch lengths) and assuming a Gaussian profile of the particle bunches. The beam induced power loss due to longitudinal impedance has been calculated for many LHC fills with both 25 ns and 50 ns bunch spacing. The calculated power losses have been compared with the measured values in the LHC. As example, Figs. 3 and 4 show the results obtained for the LHC fills 2736 (50 ns bunch spacing) and 3429 (25 ns bunch spacing). The corresponding unnormalized beam spectra are displayed in Fig. 5.

The good agreement between the expected power loss due to the impedance and the measured values with 50 ns bunch spacing (see Fig. 3) can be read as a benchmark of both the LHC beam screen impedance model and the beam

Content from this work may be used under the terms of the CC BY 3.0 licence (© 2014). Any distribution of this work must maintain attribution to the author(s), title of the work, publisher, and DOI.

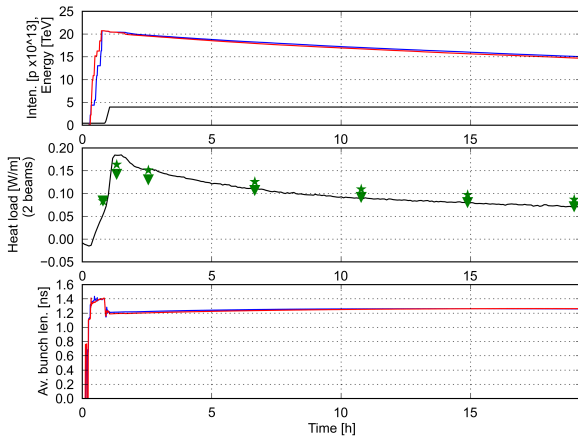


Figure 3: Top: beam energy (black) and total intensity for beam 1 (blue) and beam 2 (red) during a typical fill for luminosity production in 2012 with 50 ns bunch spacing. Middle: measured heat load in the cryogenic arcs (black), and the corresponding estimation from beam screen impedance and synchrotron radiation (stars) and only impedance (triangles). Bottom: average bunch length for the two beams.

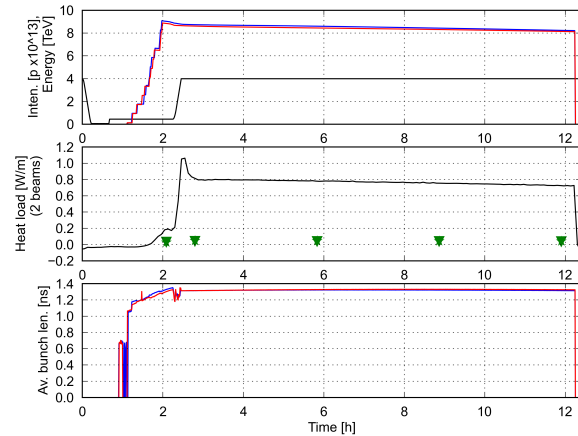


Figure 4: Top: beam energy (black) and total intensity for beam 1 (blue) and beam 2 (red) during a fill with 25 ns bunch spacing. Middle: measured heat load in the cryogenic arcs (black), and the corresponding estimation from beam screen impedance and synchrotron radiation (stars) and only impedance (triangles). Bottom: average bunch length for the two beams.

induced power loss calculations. In fact, with 50 ns bunch spacing the electron cloud is expected to play a marginal role in the beam induced power loss. On the contrary, in the case of 25 ns bunch spacing, the power loss due to the beam coupling impedance of Fig. 4 is almost negligible with respect to the measured values, because it is dominated by the electron cloud heating [5].

Power Loss in Collider's Common Chamber

For this calculation we need to generalize the power loss formula for a single beam due to a longitudinal impedance

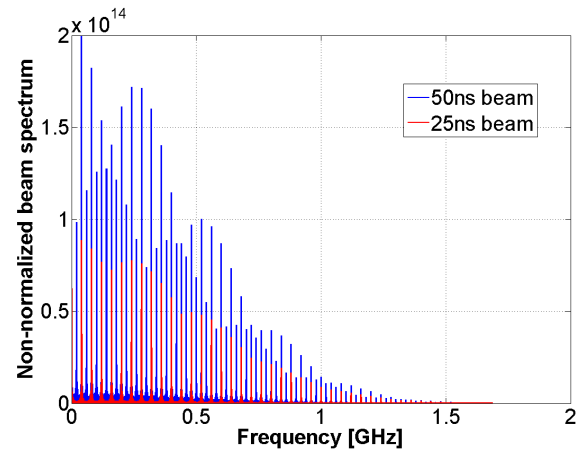


Figure 5: Calculated beam spectrum for the LHC fill 2736 (50 ns bunch spacing) and 3429 (25 ns bunch spacing).

source (see Eq. (1)) to the case of two counter-rotating beams with identical structure, going through an asymmetric chamber with offsets from the geometrical center Δy_1 and Δy_2 , respectively. At a certain longitudinal distance s from the interaction point (IP), the Beam 1 and Beam 2 signals are $\lambda_1(z) = \lambda(z)$ and $\lambda_2(z) = \lambda(z - 2s)$, respectively. The relative delay between the arrival times of the two beams at s is $\tau_s = 2s/c$ (0 at the IP and multiples of the bunch spacing at the long range encounters). The energy loss per turn of Beam 1 can be written as

$$\int_{-\infty}^{\infty} \lambda(z) \int_{-\infty}^{\infty} [\lambda(\tilde{z}) W'_{b1}(z - \tilde{z}) - \lambda(\tilde{z} - 2s) W'_{b2}(z - \tilde{z})] d\tilde{z} dz \quad (2)$$

$W'_{b1}(z)$ and $W'_{b2}(z)$ are the total longitudinal wakes per meter of beam screen at the location s from Beam 1 and Beam 2, respectively. The minus sign in front of the Beam 2 source term accounts for the counter-propagation of the beams. If, beside the order 0 longitudinal wake $W'_0(z)$, we also define the dipolar ($W'_{1d}(z)$) and quadrupolar ($W'_{1q}(z)$) components associated to excitation and witness at small offsets, respectively, the two longitudinal wakes on Beam 1 used in Eq. (2) can be expressed as

$$\begin{aligned} W'_{b1}(z) &= W'_0(z) + W'_{1d}(z) \cdot \Delta y_1 + W'_{1q}(z) \cdot \Delta y_1 \\ W'_{b2}(z) &= W'_0(z) + W'_{1d}(z) \cdot \Delta y_2 + W'_{1q}(z) \cdot \Delta y_1 \end{aligned} \quad (3)$$

Here we have introduced the first order expansion of the wakes, because due to the weld the chamber does not have a top-bottom symmetry. Due to reciprocity, it can be proven that $W'_{1d}(z) = W'_{1q}(z)$. The wakes above can be plugged into Eq. (2), providing the total energy loss per turn of Beam 1. Swapping then Beam 1 with Beam 2 in its role of witness, the total energy loss per turn can be evaluated also for Beam 2 following the same procedure. Including the multi-turn wake effect in the integrals of the energy loss and going to frequency domain, then summing up the energy loss of Beam 1 and Beam 2, we obtain a compact analytic expression for the total heat load per meter of beam screen (acting as a localized wake, or impedance, source) at the location s :

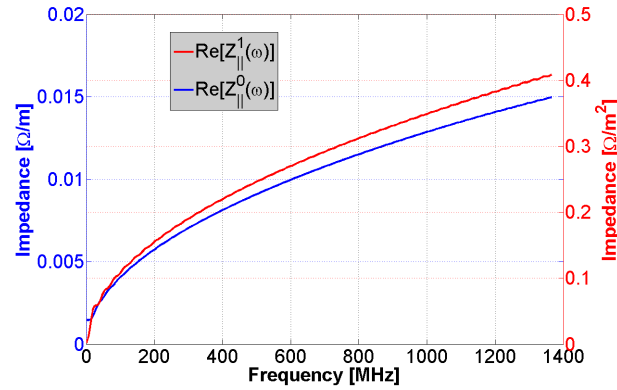


Figure 6: Real part of the impedances $Z_{||}^0(\omega)$ and $Z_{||}^1(\omega)$ for the Q2-Q3 chamber.

$$\Delta W(s) = \left(\frac{\omega_0}{\pi}\right)^2 \sum_{p=0}^{\infty} |\Lambda(p\omega_0)|^2 \left\{ \text{Re} \left[Z_{||}^0(p\omega_0) \right] + \left[\Delta y_1(s) + \Delta y_2(s) \right] \text{Re} \left[Z_{||}^1(p\omega_0) \right] \right\} (1 - \cos p\omega_0\tau_s). \quad (4)$$

Here we have defined the longitudinal impedances $Z_{||}^0(\omega)$ and $Z_{||}^1(\omega)$ of orders 0 and 1, as the Fourier transforms of the wakes defined in Eqs. 3 (and considering the equality between the dipolar and quadrupolar terms), while $\Lambda(\omega)$ is the spectrum of the signal $\lambda(z)$. The impedances have been evaluated with dedicated electromagnetic simulations of the IT beam screen, including also the effect of the weld. Sample results for the Q2-Q3 chamber are presented in Fig. 6. Therefore, to obtain the total power loss in the beam screen of the ITs, we have integrated Eq. 4 over the IT length (about 30 m between $s_0 = 23$ m and $s_1 = 53$ m) using the correct beam screen impedance model. The calculation of the heat load on the IT beam screen for a typical 50 ns fill (1374 bunches per beam, 1.6×10^{11} p/bunch) yields a value of about 4 W (i.e. an average 0.12 W/m). As we can see from Fig. 7, this is about 20 times lower than what is measured in the routine LHC operation, proving that even with 50 ns operation the IT heat load is largely dominated by electron cloud.

SUMMARY

The general calculation method of the beam induced power loss due to the beam coupling impedance has been described and applied to both single and double beam chambers. The calculated power loss in the arc beam screen

has been compared with the measured values in the LHC, showing a remarkably good agreement for beams with 50 ns bunch spacing.

A novel analytical formula for the calculation of the heat load in a collider's common chamber has been derived and applied to the LHC ITs. From this analysis we can conclude that the impedance is responsible for less than 10% of the heat load measured in the LHC ITs in 2012.

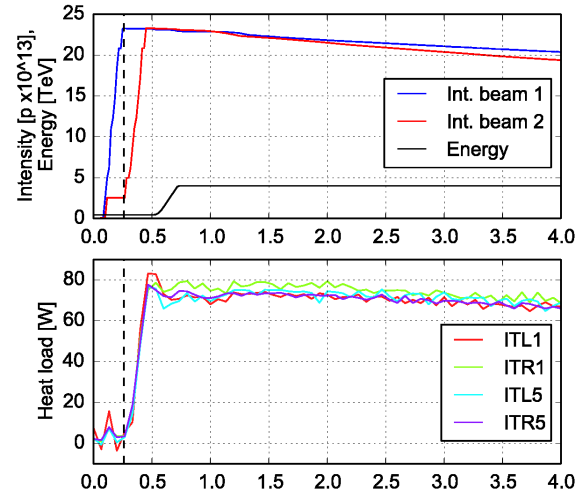


Figure 7: Beam intensity and energy (top), and heat load in the ITs around IP1 and IP5, as labeled (bottom) measured during a typical 2012 physics fill.

ACKNOWLEDGEMENTS

The measured heat load data presented in this paper are courtesy of S. Claudet and L. Tavian. Furthermore, the authors would like to thank G. Arduini, E. Métral, B. Salvant for valuable support and information.

REFERENCES

- [1] F. Ruggiero, "Single beam collective effects in the LHC", *Part. Accel*, vol. 50, pp. 83-104, 1995.
- [2] A. Mostacci, "Beam wall interaction in the LHC liner", PhD thesis, University of Rome, 2001.
- [3] www.cst.com
- [4] C. Zannini, "Electromagnetic simulation of CERN accelerator components and experimental applications", PhD thesis, Lausanne, EPFL, Switzerland, 2013.
- [5] G. Iadarola, "Electron cloud studies for CERN particle accelerators and simulation code development", PhD thesis, University of Naples Federico II, Napoli, Italy, 2014.